Heliyon 10 (2024) e36496

Contents lists available at ScienceDirect

Heliyon

journal homepage: www.cell.com/heliyon

Research article

Synthesis, characterization and As(III) scavenging behaviours of mango peel waste loaded with Zr(IV) ion from contaminated water

Deepak Gyawali [a,c], Samjhana Poudel [a], Madan Poudel [a], Kedar Nath Ghimire [a], Megh Raj Pokhrel [a], Prabin Basnet [a,b], Krishna Bahadur BK [a], Hari Paudyal [a,*]

[a] Central Department of Chemistry, Tribhuvan University, Kirtipur, Nepal
[b] Nepal Engineering College, Pokhara University, Changunarayan, Bhaktapur, Nepal
[c] Ministry of Forest and Environment, Department of Environment, Government of Nepal, Nepal

ARTICLE INFO

Keywords:
Mango peel
Zr(IV)-Loading
As(III) scavenging
Interfering ions
Desorption

ABSTRACT

Raw mango peel (RMP) was first saponified to yield saponified mango peel (SMP), which was then loaded with Zr(IV) ions to form a biosorbent for As(III) scavenging.The biosorption behaviors and mechanisms of As(III) scavenging using RMP and Zr(IV)-loaded saponified mango peel (Zr(IV)-SMP) were investigated batchwise. The As(III) scavenging efficiency of RMP increased from 20.13 % to 87.32 % after Zr(IV) loading. Optimum contact time of 6 h has been investigated for As(III) scavenging by Zr(IV)-SMP, and the data on kinetics is well fitted to the pseudo-second-order (PSO) model. Similarly, isotherm data of Zr(IV)-SMP fitted well to the Langmuir isotherm model with the maximum As(III) scavenging potential of 45.52 mg/g. Chloride (Cl^-) and nitrate (NO_3^-) have negligible influence on As(III) scavenging, but sulphate (SO_4^{2-}) interferes significantly. The exhausted Zr(IV)-SMP could be easily regenerated by treating with 2MNaOH. A mechanistic study indicates that As(III) scavenging is primarily contributed to electrostatic interaction and ligand exchange, which is confirmed from both instrumental and chemical characterizations techniques. Tubewell underground water polluted with a trace amount of arsenic (98.63 μg/L) could be successfully lowered down to the WHO standard (10 μg/L) by applying a small amount of Zr(IV)-SMP. Therefore, the Zr(IV)-SMP investigated in this work can be a low-cost, environmentally benign, and promising alternative for scavenging trace levels of arsenic from contaminated water.

1. Introduction

Contamination of waters with hazardous ions like arsenic is a major environmental concern worldwide [1]. Arsenic is a silver-grey, brittle crystalline solid that cannot be found in the earth's crust as a free element but does exist in the form of its oxoanionic form in aqueous media [2]. Natural activities such as weathering of arsenic-rich rocks, volcanic eruptions, and anthropological activities like manufacture of semiconductors, insecticide, wood preservative, paint and glass are responsible for the pollution of arsenic [3]. Groundwater is a major source of drinking water in developing countries like Nepal, India, and Bangladesh, and high concentrations of

* Corresponding author.
E-mail address: haripaudyal9@gmail.com (H. Paudyal).

https://doi.org/10.1016/j.heliyon.2024.e36496
Received 14 September 2023; Received in revised form 16 August 2024; Accepted 16 August 2024
Available online 16 August 2024

arsenic cause negative effects on human health [4]. The arsenite, arsenate, monomethylarsenate, and dimethylarsenate are the arsenic species that commonly caused toxicity in human health [5]. Trivalent arsenic, As(III), is nearly 60 times more dangerous than pentavalent arsenic, As(V), and about 100 times more toxic than the organic form of arsenic [6]. Arsenic can exist in several oxidation states (3, 0, +3, and +5), but in natural waters, it is primarily present as the inorganic oxyanions of the trivalent As(III) species (H_3sO_3 at 2–7 pH, $H_2AsO_3^-$, $HAsO_3^{2-}$ at 7–12 pH, and AsO_3^{3-}at $>$ 12 pH and penta-valent As(V) [3,6]. Diseases such as dermatitis, cardiovascular problems, diabetes, chronic bronchitis, immune disorders, peripheral nephropathy, liver damage, renal failure, adverse reproductive outcomes, hematological effects, and finally cancer may be caused by arsenic poisoning [7].

In addition to this, the people of arsenic-polluted areas are also facing social and economic troubles thesedays [2]. Around 94 to 220 million people are exposed to arsenic-contaminated groundwater, with Asia accounting for approximately 94 % of the total [2,8]. The majority of these people are from South and Southeast Asia, including India, Bangladesh, China, Nepal, and Vietnam [9]. Nepal is a landlocked country situated in southeast Asia, between China and India. It is geographically divided into three physical regions: the Mountainous or Himalayan region, the Hilly region, and the Terai region. In the Terai region, population density is high (more than 50 %), and the majority of people still rely on hand tubes and dug wells for their daily water needs, including drinking water. Arsenic pollution is prevalent in the districts of the Terai, such as Nawalparasi, Bara, Parsa, Rautahat, Rupandehi, and Kapilivastu [10]. In 1993, the World Health Organization (WHO) decreased the safe limit of arsenic concentrations from 50 μg/L to 10 μg/L because of its extreme carcinogenic behavior. Nepal is currently unable to implement the new WHO guideline due to a lack of skilled manpower, technical facilities, and economic reason, thus obeying the strict guideline limit of 50 μg/L in drinking water [11].

Nowadays, arsenic is removed from water and wastewater using a variety of methods. Some methods are oxidation/reduction, precipitation, coagulation, ion exchange, adsorption, reverse osmosis, and membrane filtration. The majority of these technologies are effective, but they are not competitive [12]. Ion exchange, reverse osmosis (RO) and membrane process are much effective technologies but are expensive for country like Nepal thus the adsorption of arsenic onto functionalized biomass materials is one of the better options. Adsorbents containing metal ions such as Fe(III), Al(III), Zr(IV) and rare earth metals are effective for arsenic treatment. Metal ions such as aluminum and iron leak easily from loaded biomass materials and are thus comparatively unsatable, whereas loading rare earth metals could potentially increase the production cost of adsorbents [5]. Zirconium and its compounds have also demonstrated a high affinity for arsenic, with the zirconia nanoparticle effectively remove arsenic from water [13]. However, due to the limited resource of Zr(IV) on the earth's surface, direct use of Zr(IV) compounds as an adsorbent for water treatment will exhaust its ore in the near future. Therefore, the development of a new material loaded with a small amount of Zr(IV), which is capable of creating the maximum number of active sites on a biodegradable polymer with its regeneration and recovery potential, is necessary for resource conservation and environmental protection.

Mango peel (MP) consist esterified pectin, cellulose, hemicelluloses, protein, polyphenolic compounds, flavonoids, xanthone c-glycosides, carotenoids, dietary fibers, and lipids, among them pectin and cellulose are major polysaccharides [14]. These polymers contain lots of functional moieties such as carboxylic acid, hydroxyl, amine, aldehyde, and so on which strongly bind metal ions. Due to the high pectin and cellulose content, MP has the potential to be used as an adsorbent for the scavenging of toxic metals, dyes, and other organic materials from industrial effluents [15]. The motives for selecting MP to fabricate a natural ligand exchanger to scavenge As(III) are: (i) functional diversity, (ii) high pectin content, (iii) easy for modification, (iv) biodegradable, and (v) abundant agricultural byproducts. Therefore, in this paper, the waste biomass of raw mango peel (RMP) was first saponified with lime water to increase the functional group density of carboxylic acid and then loaded with Zr(IV) to create ligand exchange sites for arsenic anion adsorption. The study of the interfering effect of commonly co-existing anions and suitable method of desorption for its regeneration is also systematically studied in this work.

2. Materials and methods

2.1. Materials and chemicals

Mango fruit was collected from the farmland of Kalikanagar, Butwal, Lumbini Province, Nepal. At first, the mango peel was removed from the fruits, washed, and dried. Mango peel was cut into small pieces and dried in sunlight for 7 days. The dried mango peel pieces were pulverized into powder using a mechanical grinder. Then it was sieved through a 150-μm mesh to obtain a definite particle size. It was then stored in a clean and dry polythene bottle. Sodium chloride (NaCl), calcium hydrooxide ($Ca(OH)_2$), zirconium oxychlorideoctahydrate ($ZrOCl_2{*}8H_2O$), sodium hydroxide (NaOH), hydrochloric acid (HCl), arsenic trioxide (As_2O_3), sulphuric acid (H_2SO_4), potassium dihydrogen phosphate (KH_2PO_4), sodium nitrate ($NaNO_3$), and sodium sulphate (Na_2SO_4) are the major chemicals employed in this study. All of the chemicals used in this research work are of the reagent/analytical grade and were directly employed

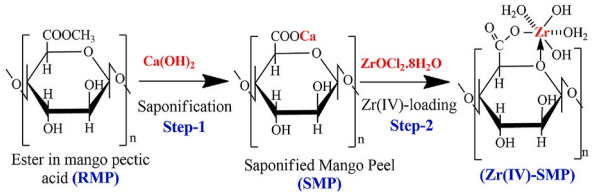

Scheme 1. Synthetic route of Zr(IV)-SMP from RMP by saponification followed by Zr(IV) loading.

without any further purification.

2.2. Preparation of Zr(IV) loaded saponified mango peel

Methyl ester part of mango pectin contained in raw mango peel (RMP) is inferred to convert carboxylic acid by treatment with base, which is popularly known as the saponification reaction. Twenty gram of RMP was first treated with 500 mL of saturated $Ca(OH)_2$ for 24 h to convert esterified pectin into a carboxylic acid group as depicted in Scheme 1 (step 1). After that, the product was filtered and washed several times with distilled water through decantation followed by filtration until a neutral pH was obtained. The product obtained was dried in a hot air oven at 60 °C for 48 h to get 8.56g of saponified mango peel (SMP), which was then subjected to Zr(IV) loading as follows. Five gram of SMP was mixed with 500 mL of a 0.1M $ZrOCl_2{*}8H_2O$ solution prepared in HEPES buffer at pH 2, and the reaction mixture was shaken for 24 h in a mechanical shaker at a speed of 180 ± 5 rpm. The reaction product obtained was filtered, washed several times with distilled water until neutral pH, and dried in an oven at 60 °C. The dried product (4.76g) obtained in this way is termed as Zr(IV)-SMP hereafter. SMP is a calcium salt of pectic acid, the loading of the Zr(IV) ion was inferred to occur with the substitution of available exchangeable calcium in SMP with Zr(IV) ion, as clearly shown in Scheme 1 (step 2).

2.3. Characterization of biosorbents

2.3.1. Boehm's titration and determination of exchangeable proton

Boehm's titration procedure described elsewhere was used to find out the amount of phenolic, lactonic, and carboxylic acid groups on the surface of Zr(IV)-SMP [16]. For this, 0.5 g of Zr(IV)-SMP was mixed with 25 mL (0.05 M each) of NaOH, $NaHCO_3$, and Na_2CO_3 in three separate bottles, then stirred for 24 h, and finally filtered. NaOH is the strongest base assumed to neutralize all Brønsted acids, while $NaHCO_3$ neutralizes carboxylic acids and Na_2CO_3 neutralizes carboxylic and lactonic groups. The filtrates were then back titrated against 0.05M NaOH with an excess of 0.05M HCl (10 mL). To determine the exchangeable proton in SMP, the SMP was first treated with 0.1M HCl at a solid-liquid ratio of 5 g/L and stirred for 24 h. After that, it was filtered, washed, and dried. The dried product (H^+-type SMP) was titrated with 0.01M NaOH and the amount of hydroxide ion consumed by SMP was determined, which is equivalent to the total amount of exchangeable protons.

2.3.2. Instrumental characterization

Fourier transform infrared (FTIR) analysis was carried out to identify the functional groups present in the feed material and their modification after saponification, Zr(IV) loading, and As(III) scavenging by using a FTIR spectrometer (IR Affinity-1S-SHIMADZU spectrometer, Kyoto, Japan). Morphological texture and elemental composition of the materials were identified using a scanning electron microscope (SEM,JEOL JSM 5900) and energy dispersive X-ray spectroscopy (EDS JEOL model JSM). Crystalline property and X-ray diffraction behavior of the samples was carried out in the range from 10 to 80 ° by using Cu-Kα (λ = 1.54056 Å) radiation using an X-ray diffractometer (Ricagu Co., Japan). The pH of the test solution was measured using a pH meter (CHEMI LINE CL-180) whereas that of arsenic concentration was measured by using atomic absorption spectrometer (PerkinElmer, USA).

2.4. Arsenic scavenging in batch mode

The effect of the pH, initial As(III) concentration, biosorbent dose, and contact times for the As(III) scavenging process were investigated batchwise. In a reagent bottle, 20 mL of pH-adjusted As(III) solution (5 mg/L) was added to 30 mg of biosorbent and shaken in a mechanical shaker for 24 h. Kinetic studies were carried out by mixing biosorbents with As(III) solution (5 mg/L) at optimum pH. Isotherm tests were carried out with different concentrations of As(III) ranging from 5 to 400 mg/L. The solutions were equilibrated for 24 h in all cases except for the kinetic studies before being filtered. The concentration of As(III) ions before and after scavenging was then determined. The effect of Zr(IV)-SMP dosage was tested by mixing 10 mL of arsenic-polluted water with different amounts of Zr(IV)-SMP ranging from 0 to 100 mg. Since chloride, nitrate and sulphate are commonly found in arsenic-polluted water [17], the interfering effect of these ions during arsenic scavenging process was determined by varying the concentration of these ions (0 mg/L to 200 mg/L) keeping As(III) concentration (1 mg/L) constant. The amount of As(III) scavenged per unit mass and percentage scavenging are calculated by using equation (1) and equation (2) [2,6].

$$q = \frac{C_i - C_e}{W} \times V \tag{1}$$

$$\%\, A = \frac{C_i - C_e}{C_i} \times 100 \tag{2}$$

Where,C_i and C_e (mg/L) are adsorbate concentrations before and after scavenging As(III), respectively,V (L) is the volume of As(III) solution, and W (g) is the weight of biosorbent used.

2.5. Desorption of scavenged arsenic

For this, As(III)-loaded Zr(IV)-SMP was first prepared by mixing 500 mL of As(III) solution (100 mg/L at pH 10.18) with 2.14g of Zr (IV)-SMP and stirring for 24 h. Then it was filtered, and the residue was collected, washed until neutral pH, and dried in a hot air oven

at 60 °C for 48 h. The dried product obtained from this reaction is termed As(III)-loaded Zr(IV)-SMP and abbreviated as As–Zr(IV)-SMP hereafter. A preliminary desorption test was carried out using acidic (1M HCl), neutral (1 M NaCl), and basic (1M NaOH) solutions at a solid-liquid ratio of 5 g per liter. NaOH showed effective desorption of scavenged As(III) compared to HCl and NaCl. Therefore, optimization of NaOH solution was done by shaking 30 mg of As–Zr(IV)-SMP with 10 mL of NaOH solution at different concentration (0.05–2.0M). The efficiency of arsenic desorption was determined by analyzing the arsenic in desorbed solution and the percentage desorption was calculatedas [18,19].

$$\%D = \frac{D_A}{A_A} \times 100 \tag{3}$$

Where A_A and D_A are the amounts adsorbed or scavenged and dessorbed expressed as mg/g of As(III) ions, respectively.

3. Results and discussion

3.1. Chemical modification of RMP and creation of active sites

Methylated ester groups exist in RMP are considered to be converted into carboxylic acids after saponification reaction and produced calcium salt of mango pectic acid. It contains exchangeable calcium (Ca(II)) and acts as cation exchanger where active sites for As(III) scavenging are created by Zr(IV) loading. The details of Zr(IV) loading and creating active sites for As(III) anions is explain as follows. Tetravalent zirconium, Zr(IV), ions generally forms the octahedral complex in an aqueous solution and the loading of Zr(IV) occurred by the substitution of calcium from SMP. Due to big polymeric structure of mango pectic acid in SMP, neutralization of all 4 positive charges of Zr(IV) by carboxylic acid groups of SMP is impossible due to the steric hindrance during Zr(IV) loading. Thus one or two positive charges of Zr(IV) are neutralized by pectic acid groups of SMP, rest are neutralized by hydroxyl or chloride ions existed in the aqueous solution, and other oxidation numbers are fulfilled by water ligands.

3.2. Characterizations of biosorbents

3.2.1. Distributions of various elements and EDS spectra

To investigate the existence of various elements and their distributions, EDS mapping of feed material (RMP), Zr(IV)-SMP, and As (III)-loaded Zr(IV)-SMP was done, and the observed results are presented in Fig. 1 and Supplementary Fig. S1). The elemental distribution shows that carbon (red) and oxygen (dark green) are homogeneously distributed on the surface of RMP (Fig. 1(A)), whereas sodium (light blue), magnesium (dark blue), silicon (grey), potassium (purple), and calcium (light green) are distributed heterogeneously. It is evident from the elemental mapping of Zr(IV)-SMP (supplementary figure, S1) that zirconium (light green), chlorine (blue), oxygen (green), and carbon (red) are major elements in Zr(IV)-SMP. New elements zirconium (Zr) and chlorine (Cl) were

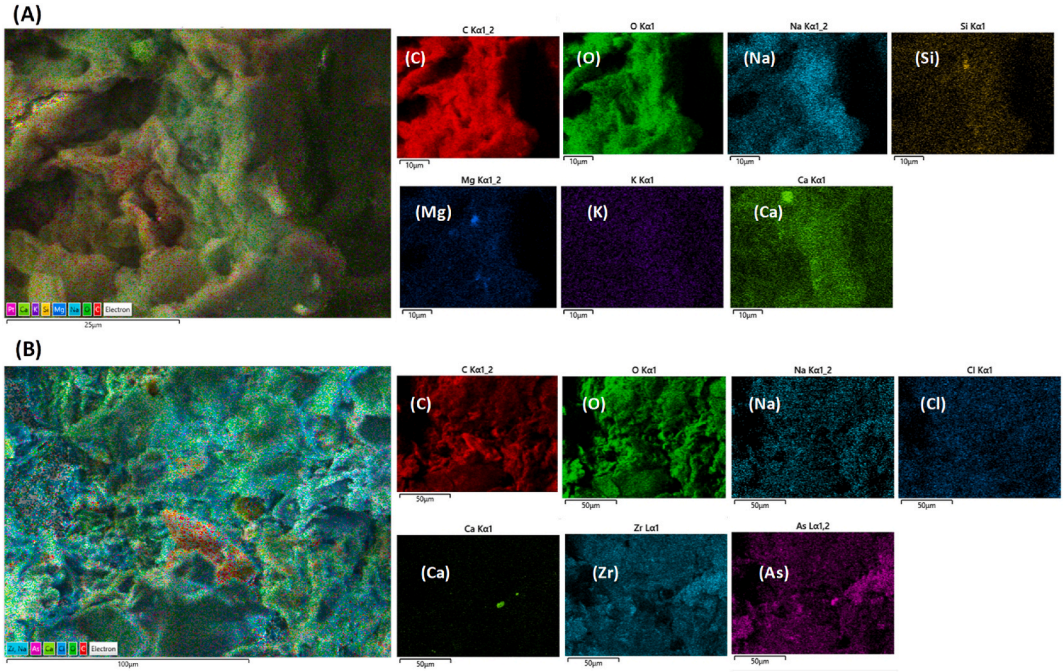

Fig. 1. Elemental distribution and mapping of individual elements in (A) RMP and, (B) Zr(IV)-SMP after As(III) scavenging.

observed in Zr(IV)-loaded SMP which are absent in RMP (feed material), it is due to the loading of Zr(IV) by treating SMP with $ZrOCl_2.8H_2O$ solution. After As(III) scavenging (Fig. 1(B)), elements such as carbon (red), oxygen (green), sodium (blue), chlorine (dark blue), calcium (dark green), zirconium (light blue), and arsenic (purple) are observed. The existence of arsenic in Zr(IV)-SMP after As(III) scavenging provides direct evidence of As(III) biosorption onto Zr(IV)-SMP surface.

EDS spectra of RMP, Zr(IV)-SMP, and As(III)–Zr(IV)-SMP are shown in Supplementary Figs. 2–4 (S2–S4), respectively.The atomic percentages of various elements in Zr(IV)-SMP are: carbon (64.30 %), oxygen (30.85 %), chlorine (0.95 %), calcium (0.03 %), and zirconium (3.87 %), whereas in the case of As(III)–Zr(IV)-SMP, they are: carbon (62.88 %), oxygen (31.86 %), sodium (0.04 %), chlorine (0.21 %), calcium (0.05 %), zirconium (3.73 %), and arsenic (1.22 %). It shows that the weight percentage of oxygen (O) and arsenic (As) increased after As(III) scavenging. It strongly suggested that the complex ion containing arsenic and oxygen is adsorbed on the surface of Zr(IV)-SMP during As(III) scavenging process. All the results from the EDS analysis provided clear and direct evidence that Zr(IV)-SMP successfully scavenged oxyanions of As(III) from water.

3.2.2. Modification of functional groups and crystalline property of biosorbent

FTIR analysis was carried out to identify the functional groups that existed in feed material (RMP) and their modification after saponification, Zr(IV) loading, and As(III) scavenging. FTIR spectra of RMP, SMP, Zr(IV)-SMP, and As–Zr(IV)-SMP in the range from 400 to 4000 cm^{-1} are shown **in** Fig. 2(A)–2(C). The broad peak at 3200 to 3600 cm^{-1} in RMP indicates the presence of OH groups [20]. The peaks at 1700–1900 cm^{-1} and 1600–1700 cm^{-1} suggest the existence of C=O and C–O stretching, respectively.The peak centered around 1400 cm^{-1} and 1000 cm^{-1} corresponds to the aliphatic and aromatic C–H and the C–O groups in alcohol, carboxylic acid, and

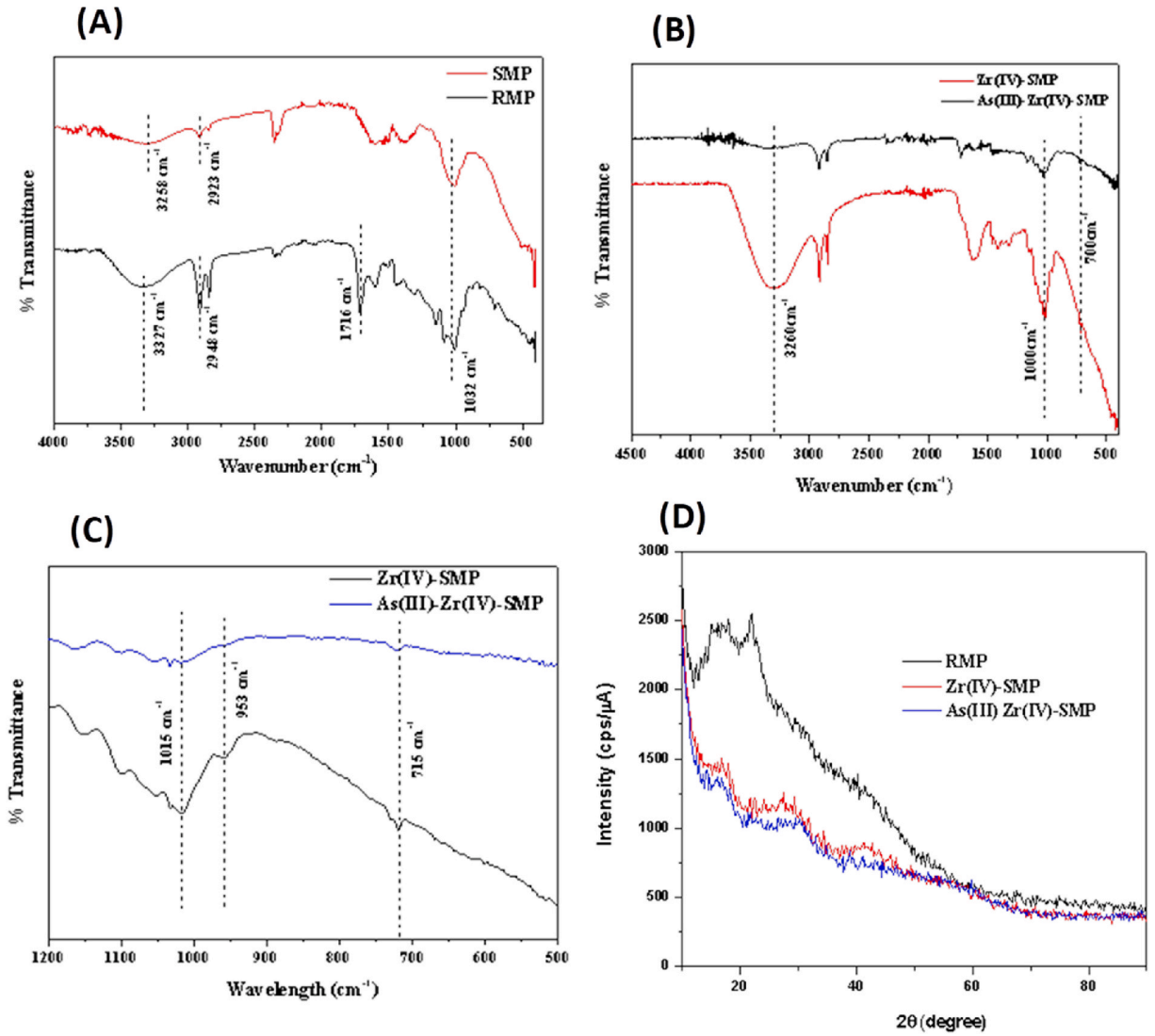

Fig. 2. FTIR spectra and XRD patterns of biosorbent showing functional groups and crystallinity change.

ether (C–O–C) [21]. The peak at 1716 cm^{-1} due to C=O stretching of mango pectic acid in RMP was found to disappear in the saponified product (SMP) due to the formation of calcium salts of carboxylic acid called calcium pectate (Fig. 2(A)) and Zr(IV) pectate in Zr(IV)-SMP (Fig. 2(B)). Two peaks centered at 1635 cm^{-1} and 1436 cm^{-1} in RMP correspond to stretching vibrations of ionic carboxylic groups, which were shifted to 1610 cm^{-1} and 1427 cm^{-1} in the case of SMP and 1602 cm^{-1} and 1420 cm^{-1} in the case of Zr (IV)-SMP, respectively. It provides strong evidence that carboxylic acid groups were principally involved in saponification and Zr(IV) loading reactions. After As(III) scavenging, the –OH stretching vibration observed at 3260 cm^{-1} in Zr(IV)-SMP gets weakened, which is attributed to the reduction of the –OH group after As(III) scavenging. The pH of the arsenic solution was found to be increased after As (III) scavenging, which also provides the evidence of releasing hydroxyl ions, which will be described in detail in a later section. For more clearance, the FTIR spectra of Zr(IV)-SMP and As–Zr(IV)-SMP were plotted between 1200 and 500 cm^{-1}, as shown in Fig. 2(C). A sharp peak observed at 953 cm^{-1} in Zr(IV)-SMP is attributed to the vibration of the Zr–O bond. Moreover, a new peak corresponding to As–O observed at a wavelength of around 715 cm^{-1} in the case of As–Zr(IV)-SMP, which provided the clear evidence that As(III) is effectively scavenged onto the functional groups of Zr(IV)-SMP.

The XRD patterns of RMP, Zr(IV)-SMP, and As–Zr(IV)-SMP are shown in Fig. 2(D). It is observed from this result that the feed material (RMP) has a crystalline structure due to the existence of sharp peaks at 2θ around 16 and 21°. However, in the case of Zr(IV)-SMP, two broad and characteristic amorphous bands of zirconium oxide appeared at 2θ around 18–27° and 29–34°, which provided the evidence that crystalline RMP is converted into amorphous Zr(IV)-SMP. A slight change in the position of the peak occurred after As (III) scavenging. The intensity of some peaks decreased, while some peaks disappeared, and some new peaks appeared which might be due to the conversion of adsorbed arsenic into arsenic oxide at 2θ around 15, 19, 45, and 50° [22]. It confirmed that the crystalline properperty of the RMP drastically changed after chemical modification and produced amorphous Zr(IV)-SMP, where adsorption of As (III) is much favoured than RMP.

3.2.3. *Morphological characteristics of biosorbents*

The surface morphology of the biosorbents is supposed to be changed after chemical modification and As(III) scavenging. To investigate this, FE-SEM images of RMP, SMP, Zr(IV)-SMP, and As–Zr(IV)-SMP were recorded, and the results are presented in Fig. 3. The surface of RMP (Fig. 3(A)) is a little bit waxy and contains an oily layer with some white patches, which may be due to the existence of pigments (like limonene and chlorophyll), water-soluble sugar, and minerals. After $Ca(OH)_2$ or base treatment, the surface became much zig-zac as shown in Fig. 3(B), which may be due to the dissolution of soluble organic compounds such as sugar, citric acid, limonene, and other minerals. The surface morphology became much changed after Zr(IV) loading, the large ups and downs observed in SMP were diminished (Fig. 3(C)), which is attributed to the surface coverage of SMP by Zr(IV) ion. After As(III) scavenging (Fig. 3 (D)), the surface of the Zr(IV)-SMP becomes a little bit distrubed, where some irregular layers of As(III) on the Zr(IV)-SMP surface are observed. It might be due to the scavenging of As(III) onto the surface of Zr (IV)-SMP.

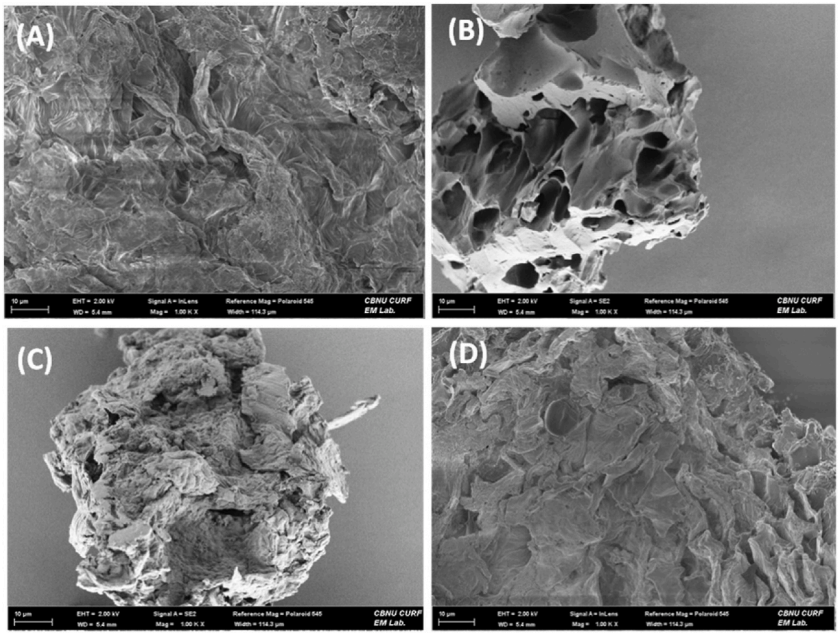

Fig. 3. FE-SEM images of (A) RMP, (B) SMP, (C) Zr(IV)-SMP, and (D) Zr(IV)-SMP after As(III) uptake.

3.3. Batch-wise scavenging of As((III) ion

3.3.1. Effect of pH and As(III) scavenging mechanism

The primary pH dependent factors for As(III) scavenging are the surface charge of the adsorbent and the As(III) speciation in water. For scavenging As(III), the pH is a key controlling factor because the solubility of metal ions, the concentration of counter ions on the functional groups of the biosorbent, and the degree of ionization of the adsorbate are influenced by pH [23]. Fig. 4 shows the % scavenging of As(III) onto RMP and Zr(IV)-SMP as a function of equilibrium pH. It is observed from the result of this figure that RMP showed a lower scavenging percentage (2.72 %) even at an optimal equilibrium pH of 8.37. However, the Zr(IV)-SMP showed a dramatic improve of As(III) scavenging percentage (87.32 %) at pH 10.18. Moreover, an aqueous solubility of RMP was visibly observed from our naked eyes, which potentially increases the TOC level in treated water and interferes the As(III) scavenging process. Utilization of RMP as biosorbent material for As(III) scavenging is not appropriate in terms of economic benefit and environmental prospects thus further study were carried out with Zr(IV)-SMP only. Moreover, the result also reveals that the % scavenging of As(III) is lower at lower pHs, whereas it is significantly increased at pHs higher than 8 and reached maximum value at pH 10.18 by using Zr (IV)-SMP.

From As(III) speciation in aqueous medium, neutral species of As(III) (H_3AsO_3) are major species at pH below 9 whereas mono-anionic ($H_2AsO_3^-$) species are predominant from 9 to 12 pH [24]. The maximum As(III) scavenging is observed at pH 10.18; thus the majority of scavenging occurred in the form of $H_2AsO_3^-$ ions. Small amount of As(III) is also scavenged at pH below 9, where its scavenging occured in the form of neutral H_3AsO_3. The result indicated that both neutral as well as anionic specicies of As(III) are scavenged using Zr(IV)-SMP adsorbent. The coordinated hydroxyl/ or chloride (OH/or Cl) ligands and water (H_2O) ligands exists in the coordination sphere of loaded Zr(IV) in Zr(IV)-SMP are the main active sites for the scavenging of As(III) anion from water *via* ligand exchange mechanisms as demonstrated in Scheme 2. The low scavenging percentage of As(III) observed at lower pHs (acidic pH, i.e., pH 1–6) is due to the existence of neutral species of the As(III) as the dominant species which are hardly adsorbed onto Zr(IV)-SMP. At optimum pH *(i.e.* pH = 10.18), the predominant species is $H_2AsO_3^-$, which is easily exchanged with Cl/or OH ligands of Zr(IV)-SMP by ligand substitution reaction as clerely depicted in Scheme 2, resulting in a higher scavenging percentage. At a higher pH (>11), the percentage scavenging of As(III) decreased with a further increase in equilibrium pH, which might be due to the competition of hydroxyl ions with As(III) anion for the same scavenging sites. A similar ligand exchange type As(III) adsorption behavior was also observed by Biswas et al. using Zr(IV)-loaded saponified orange waste [25].

3.3.2. Effect of contact time for As(III) scavenging

Fig. 5(A) shows the effect of contact time on the scavenging behavior of As(III) ions. It shows that As(III) scavenging rate is higher at the beginning as there are a large number of scavenging sites. The rate gradually decreases and reaches equilibrium at 6 h, after which there is no significant increase in the As(III) scavenging rate occurs. This is because of the fact that the As(III) scavenging sites in Zr(IV)-SMP were nearly occupied. The scavenging rate is proportional to the number of vacant sites on the biosorbent surface [26]. Although equilibrium was achieved within only 6 h, the solid-liquid mixture in other experimental works was stirred for 24 h to ensure complete equilibrium. The pseudo-first-order (PFO), and pseudo-second-order (PSO) kinetic models were used to investigate the best fit model during As(III) scavenging by Zr(IV)-SMP. Non-linear and linear equations for PFO (Eqs. (4) and (5)), and PSO models (Eqs. (6) and (7)) are respectively expressed as [27].

PFO model:

$$q_t = q_e\left(1 - e^{-k_1 t}\right) \tag{4}$$

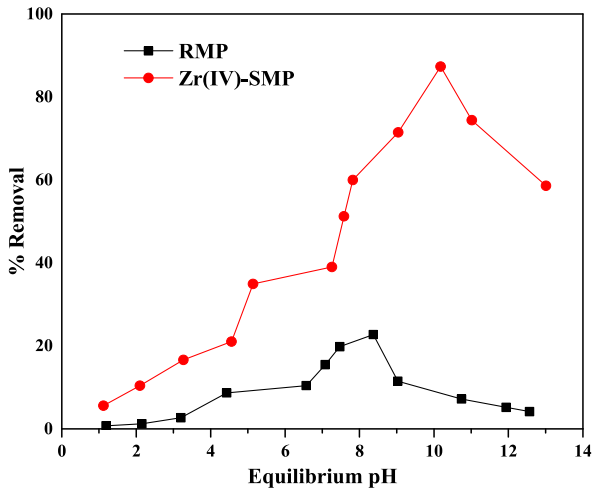

Fig. 4. Effect of pH for the uptake of As(III) onto RMP and Zr(IV)-SMP.

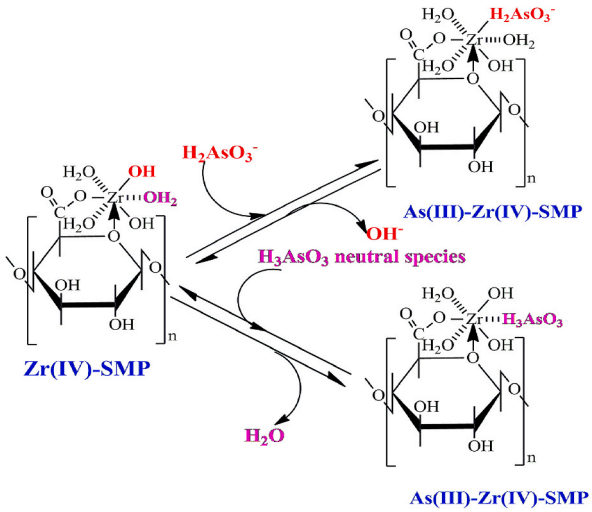

Scheme 2. Possible ligand exchange mechanism for As(III) onto Zr(IV)-SMP.

$$\log(q_e - q_t) = \log q_e - \frac{k_1}{2.303}t \tag{5}$$

PSO model:

$$q_t = \frac{k_2 {q_e}^2 t}{1 + k_2 q_e t} \tag{6}$$

$$\frac{t}{q_t} = \frac{1}{k_2 {q_e}^2} + \frac{1}{q_e}t \tag{7}$$

Where,q_e and q_t are the As(III) biosorption capacity at equilibrium and at time t, respectively and k_1 and k_2, are respective values of rate constant for PFO and PSO.

The linear or straight line for the PFO model is obtained by plotting log(q_e-q_t) *versus* time (Fig. 5(B)), whereas the PSO model is obtained from the plot of t/qt *versus* time (Fig. 5(C)). The straight-line plots obtained from both isotherm models are used for the determination of isotherm parameters, and the calculated parameters are listed in Table 1. The result shows that the coefficient of determination for the PSO model (R^2 = 0.99) is higher than that of the PFO model R^2 = 0.88). The As(III) scavenging capacity determined using the PSO model (2.58 mg/g) is very much closer to the experimentally determined scavenging capacity (2.50 mg/g); however, it is far from the experimental value in the case of the PFO model (1.68 mg/g). This result strongly suggested that the As(III) scavenging using Zr(IV)-SMP strictly follows PSO kinetics.

For further evidence, the experimental data were subjected to non-linear fitting. The kinetic parameters obtained from linear fitting were used to determine the As(III) scavenging capacities at different time intervals and plotted together with experimental data as shown in Fig. 5(A). The value of As(III) uptake capacity (q_e) determined from the non-linear fitting of the PSO kinetic model agreed better with the experimental uptake capacity (q_e) compared to As(III) uptake capacity (q_e) determined using the PFO model. Therefore from all of these findings, it is confirmed that the scavenging kinetics of As(III) follow the PSO kinetic with the chemisorption mechanism.

3.3.3. *As(III) scavenging isotherm*

Fig. 6(A) shows the relationship between the As(III) uptake capacity of Zr(IV)-SMP as a function of equilibrium concentration. The result demonstrates that the scavenging of As(III) onto Zr(IV)-SMP increases as the equilibrium concentration of As(III) ions increases, then reaches a plateau value at higher concentrations. When the equilibrium concentration increased from 5.15 to 356.49 mg/L, the As (III) scavenging capacity increased from 2.52 to 34.52 mg/g. The mass transfer driving force increased with the increase in As(III) concentration, which thereafter enhanced the concentration gradient. Hence, a large number of As(III) ions move from the bulk of the solution to the surface of Zr(IV)-SMP that finally increases the As(III) scavenging capacity [28]. The formation of the plateau at higher concentrations is the characteristic of Langmuir-type monolayer formation, which will be further proved by isotherm modeling as follows. Two isotherm models, namely the Langmuir and the Freundlich, are employed here to analyze the experimental data of As(III) scavenging by Zr(IV)-SMP. Non-linear and linear equations for the Langmuir isotherm (Eqs. (8) and (9)) [29], and the Freundlich isotherm models (Eqs. (10) and (11)) [30] can be expressed as.

Langmuir isotherm model

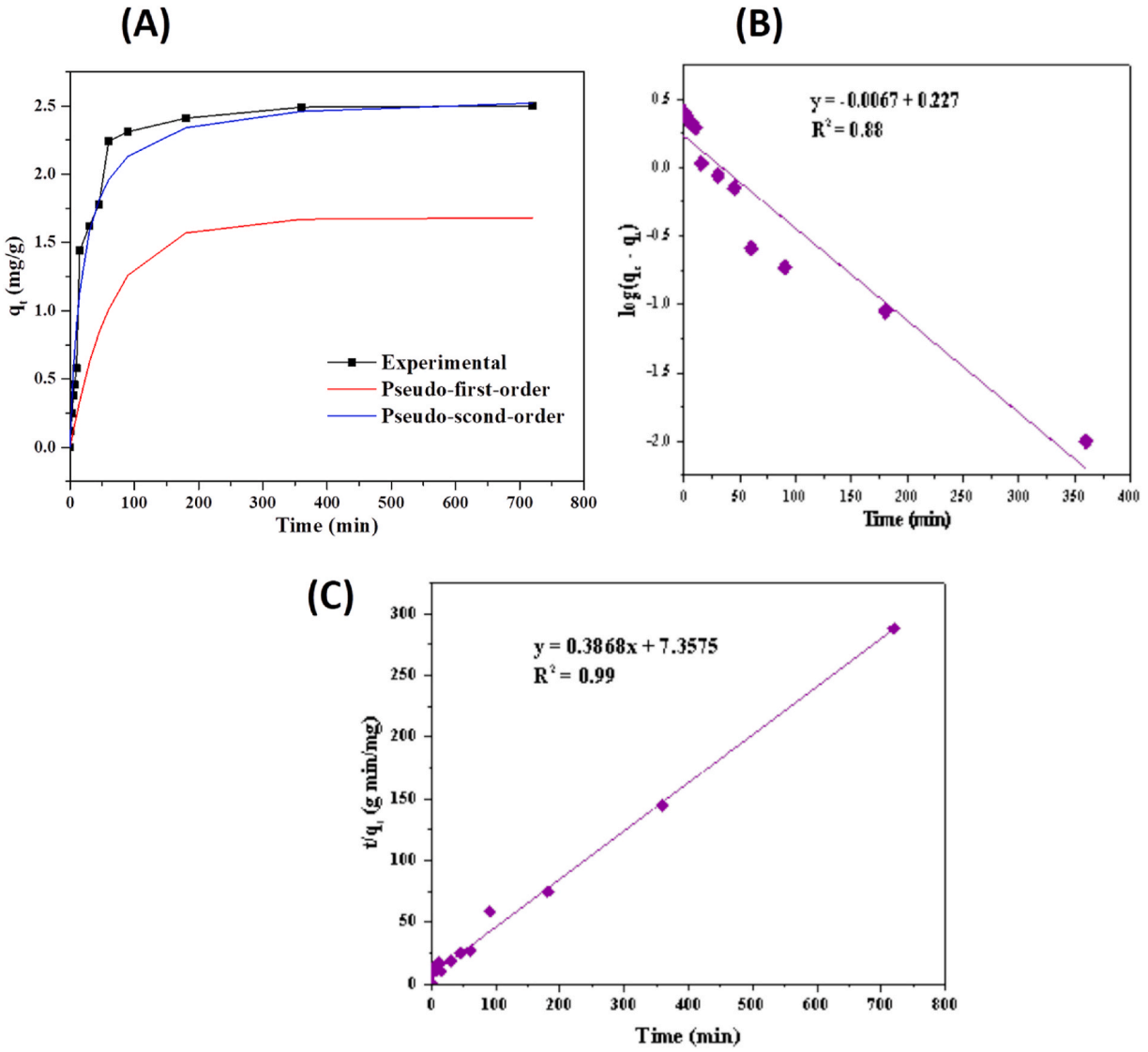

Fig. 5. Bio-scavenging kinetics of As(III) using Zr(IV)-SMP from aqueous medium.

Table 1
Experimental and calculated kinetic parameters for scavenging of As(III) onto Zr(IV)-SMP.

Kinetic models	Evaluated kinetic parameters	Zr(IV)-SMP
Pseudo-first order (PFO)	k_1 (1/min)	0.015 ± 0.007
	q_e, cal. (mg/g)	1.68 ± 0.103
	q_e, exp. (mg/g)	2.46 ± 0.43
	R^2	0.88
	χ^2	0.36 ± 0.023
	RMSE × 10^{-2}	0.26 ± 0.005
Pseudo-second order (PSO)	k_2 (g/mg min)	0.020
	q_e, cal.(mg/g)	2.58 ± 0.32
	R^2	0.99
	q_e, exp. (mg/g)	2.46 ± 0.43
	χ^2	0.56 ± 0.065
	RMSE × 10^{-2}	0.04 ± 0.007

$$q_e = \frac{q_{max}\, b\, C_e}{1 + bC_e} \quad (8)$$

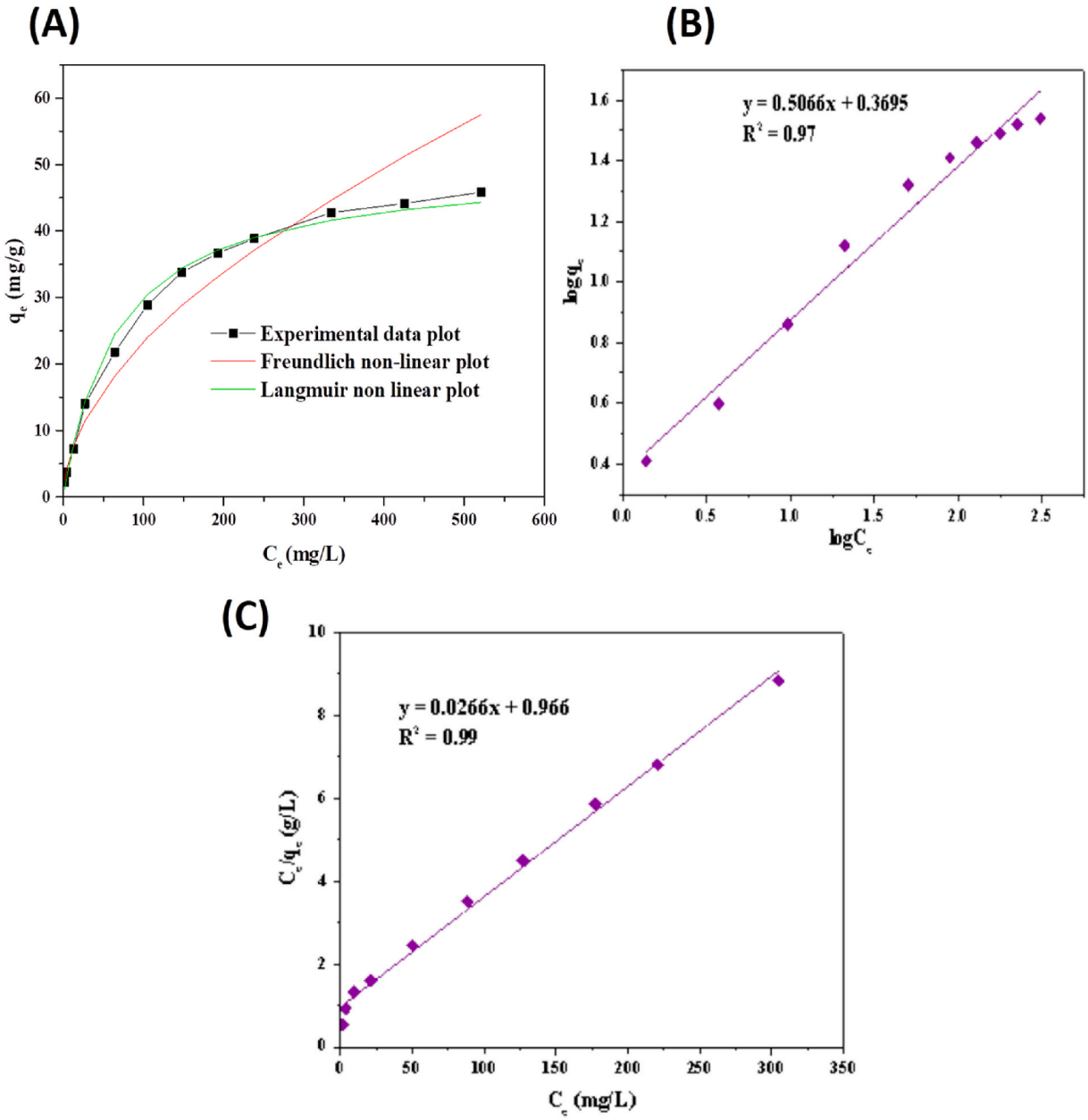

Fig. 6. Bioscavenging isotherm of As(III) using Zr(IV)-SMP (A) experimental plot, (B) Friendlich isotherm plot, and (C) Langmuir isotherm plot.

$$\frac{C_e}{q_e} = \frac{1}{q_{max}\, b} + \frac{1}{q_{max}} C_e \tag{9}$$

Freundlich isotherm model

$$q_e = K_F C_e^{1/n} \tag{10}$$

$$\log q_e = \log K_F + (1/n) \log C_e \tag{11}$$

where q_e (mg/g) and q_t (mg/g) are the As(III) uptake capacity at equilibrium time and at time t, respectively, and q_{max} (mg/g) is the maximum As(III) scavenging capacity of the investigated biosorbent. The constant b is the Langmuir equilibrium constant related to binding energy, whereas K_F is the Freundlich constant representing the intensity of adsorption. The Langmuir isotherm is obtained by plotting C_e/q_e against C_e (Fig. 6(B)), and the Freundlich isotherm is obtained by plotting log(q_e) against log(C_e) (Fig. 6(C)). Linear plots

are obtained from both models, and the isotherm parameters obtained from both isotherm models are listed in Table 2. The coefficient of determination in the case of the Langmuir isotherm model ($R^2 = 0.99$) is higher than the Friendlich isotherm model ($R^2 = 0.97$), which indicates that the experimental data is more closely fitted to the Langmuir isotherm than the Freundlich isotherm, depicting the homogeneous distribution of active sites resulting in the formation of a monolayer of As(III) ions on the surface of Zr(IV)-SMP as described by Langmuir theory [31]. The value of 1/n from the Freundlich model is obtained in the range between 0 and 1, which suggested that the As(III) scavenging process using Zr(IV)-SMP is favorable. To further confirmation, the experimental data were analyzed using the non-linear equations of the Langmuir and the Freundlich isotherm models. The As(III) uptake capacity determined from non-linear modelling for each concentration is plotted together with experimental data as illustrated in Fig. 6(A). The results showed that the As(III) uptake capacity determined from the non-linear fitting of the Langmuir isotherm model closely resembled with the experimental data of As(III) uptake capacity compared to Friendlich model. All of these facts indicate that the As(III) scavenging onto Zr(IV)-SMP occurred similar to the monolayer adsorption of gas on the surface of solid as described by Langmuir in 1916 [29].

The comparative study regarding the As(III) scavenging potential of investigated Zr(IV)-SMP with the maximum uptake capacity of other biosorbents reported in the literature was done and presented in Table 3 [25,23,32–44]. The results revealed that non-modified biomass such as tea waste, fungus, fish scale, biotite, and *Morus alba* leaves have low scavenging potential, whereas metal-loaded biosorbents, especially Zr(IV)-loaded orange waste, Zr(IV)-loaded polyacrylamide hybrid material, and other biosorbents loaded with rare earth metals possess a high potential for As(III) scavenging. Zr(IV)-SMP biosorbent investigated in the present work has satisfactory As(III) scavenging potential compared to the majority of the biosorbents reported in the literature. In addition to this the feed material for the production of Zr(IV)-SMP is waste material itself therefore, the Zr(IV)-SMP investigated in this work can be an efficient, low-cost, and environmentally benign adsorbent for the remediation of arsenic from arsenic-contaminated water.

3.3.4. Effect of interfering ions

The arsenic-polluted water not only contains arsenic but also has other interfering anions such as chloride (Cl^-), sulphate (SO_{42}^-), and nitrate (NO_3^-) in nature [45]. Arsenic forms inner-sphere complexes with these co-existing anions, reducing the interaction between the two anions. The effects are more pronounced with the change in pH and concentrations [46]. To know the influence of these anions on the scavenging of As(III), their interfering effects should be known so that the influence of As(III) scavenging by investigated Zr(IV)-SMP in the co-existing system was studied at different concentrations and the results obtained are shown in Fig. 7. The order of interference observed is as follows: sulphate > nitrate > chloride. The reduction of the As(III) scavenging percentage of Zr(IV)-SMP in the presence of these co-exisiting ions is due to the interference with the As(III) anions caused by the competition with As(III) for the same scavenging site [47]. The results reveal that the sulphate caused the strongest interfering effect compared to the chloride and nitrate, which may be due to the existence of more negative charge (di-anionic nature) and higher stability of sulphate and zirconium (Zr^{4+}-SO_4^{2-}) bond with loaded Zr(IV) in Zr(IV)-SMP.

3.3.5. Desorption of loaded As(III)

To identify the excellent desorbing solution, the preliminary desorption test was carried out by using 1M NaOH (basic solution), 1M HCl (acidic solution), and 1M NaCl (neutral solution) at a solid-liquid ratio of 5 g/L. From this, it was found that NaOH is more effective than HCl and NaCl. Only 18.37 % of As(III) was desorbed by NaCl, whereas HCl caused the trouble of Zr(IV) leaching from Zr(IV)-SMP. Thus, these chemicals are not suitable desorbents. 1M NaOH desorbed 81.35 % of As(III). Thus, optimization of the eluent solution was done using NaOH at different concentrations. Fig. 8 shows the %desorption of As(III) from As(III)–Zr(IV)-SMP at a solid-liquid ratio of 5 g/L using different concentrations of NaOH. The experimental results showed that the desorption percentage increased from 10.7 % to 81.35 % on increasing the molar concentration of NaOH from 0.05 to 1M, and the highest percentage of As(III) desorption (94.30 %) occurred using 2M NaOH. Therefore, 2M NaOH solution can be an optimum concentration of NaOH for effective desorption of adsorbed As(III) ion from As(III)–Zr(IV)-SMP. It is inferred that NaOH provided hydroxyl ions in an aqueous medium, which is supposed to be replaced or substituted by the As(III) anion from As(III) adsorbed Zr(IV)-SMP during the desorption process, as depicted in Scheme 3.

Table 2
Models and experimental parameters of isotherm for scavenging of As(III) by Zr(IV)-SMP.

Isotherm models	Evaluated isotherm parameters	Zr(IV)-SMP
Langmuir isotherm	$q_{m,\ exp}$(mg/g)	44.18 ± 1.27
	$q_{m,cal.}$ (mg/g)	45.34 ± 2.63
	b (L/mg)	0.026 ± 0.0034
	R^2	0.99
	χ^2	0.029 ± 0.0052
	RMSE	0.38 ± 0.017
Freundlich isotherm	K_F (mg/g)	2.32 ± 0.48
	n	2.70 ± 0.85
	R^2	0.97
	χ^2	755.28 ± 9.38
	RMSE	13.95 ± 1.29

Table 3
Comparison of arsenic scavenging capacities of various biosorbents with investigated Zr(IV)-SMP.

Adsorbents	Arsenic species	q_{max} (mg/g)	pH	References
Zr(IV)-SMW	**As(III)**	**45.34**	**10.18**	**This study**
Zirconium oxide nanoparticles	As(III)	83.2	7.0	[13]
Zr(IV) loaded SOW	As(III)	130	10.0	[20]
La(III)-SWR	As(III)	37.73	12.0	[24]
Iron Nano Bio-composite	As(III)	1.04	6.0	[33]
Powdered almond shell (ALS)	As(III)	4.6	7.2	[34]
Citrus limetta PAC – 500	As(III)	0.72	3.0	[35]
Citrus limetta PPAC - 500	As(III)	0.53	3.0	[35]
Bacillus thuringiensis strain WS3	As(III)	10.94	7.0	[36]
Zr(IV)-polyacrylamide hybrid material	As(III)	41.48		[37]
Magnetic Nanocomposite	As(III)	28	2.9	[38]
Pinecone Magnetite composite	AS(III)	16.8	8.0	[39]
Modified hazelnut shell	As(III)	11.84	9.0	[40]
Iron Coated seaweeds	As(III)	4.2	7.0	[41]
Iron-doped amino-functionalized sawdust	AS(III)	10.1	7.0	[42]
ZrO_2 coated sawdust	AS(III)	29	7.0	[43]
La_2O_3 coated sawdust	As(III)	22	7.0	[43]
Dried fine powdered biomass of *Momordica charantia*	As(III)	0.88	9.0	[44]

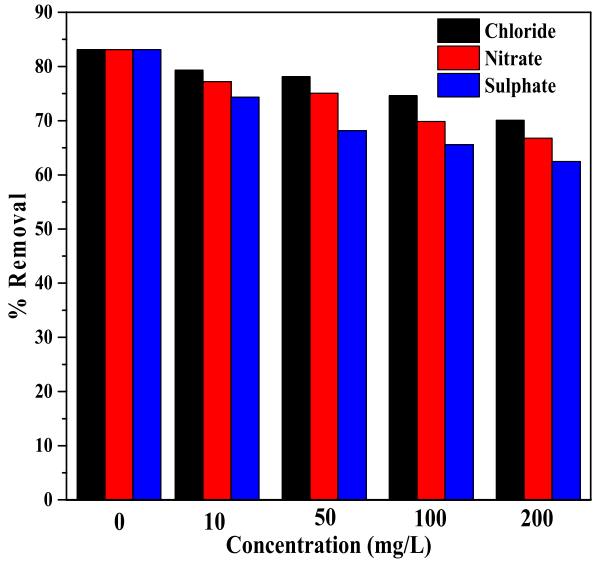

Fig. 7. Effect of interfering anions on the scavenging of As(III) by Zr(IV)-SMP.

3.4. Application of investigated Zr(IV)-SMP for the treatment of arsenic-polluted water

The public health in the Terai region is seriously threatened by arsenic contamination of the groundwater. The southwest to southeast region of Nepal, particularly Sunsari, Saptari, Siraha, Dhanusha, Sarlahi, Rautahat, Bara, Nawalparasi, Rupandehi, Kapilbastu, Banke, Kailali, and Kanchanpur, have recently become a major concern due to high levels of arsenic in groundwater [10]. Arsenic contamination of groundwater at levels greater than 50 μg/L continues to have a detrimental effect on human beings.We have gathered the arsenic-contaminated water from the Lumbini province of Nepal's Nawalparasi district. This contaminated water initially had 98.63 μg/L of arsenic, which is about 9.8 and 1.96 times higher than the WHO and Nepalese drinking water guideline levels, respectively [11].

The residual concentration of arsenic as a function of Zr(IV)-SMP dosage is depicted in Fig. 9. It reveals that using only 1.5 g/L of Zr (IV)-SMP for tested arsenic polluted groundwater sample lowered arsenic concentration levels less than the Nepalese drinking water standard (50 μg/L), and its level is further lowered with the increase of Zr(IV)-SMP amount. More intrestingly, the tested Zr(IV)-SMP effectively reduced the arsenic concentration below the WHO recommended threshold limit (10 μg/L) by using higher than 2.5 g/L, and 100 % removal of arsenic from contaminated water can be achieved by using 6.25 g/L of Zr(IV)-SMP. As a result, it can be claim that the investigated Zr(IV)-SMP could be an excellent material as high capacity, environmentally benign, and economic alternative for the removal of trace amounts of arsenic from contaminated water.

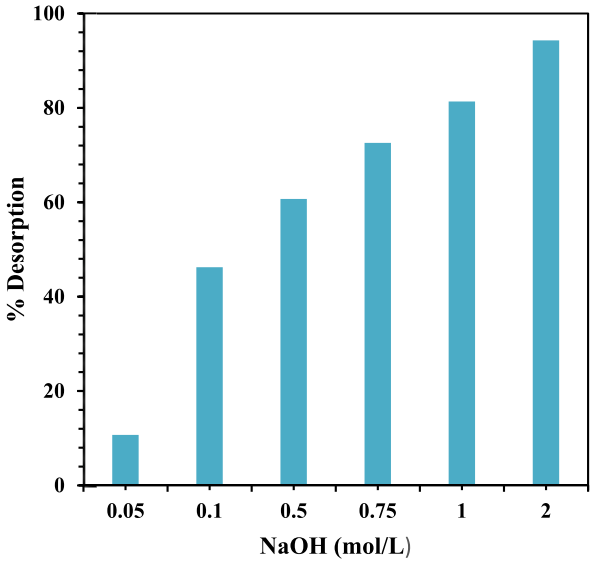

Fig. 8. Desorption percentage of As(III) as a function of molar concentration of NaOH.

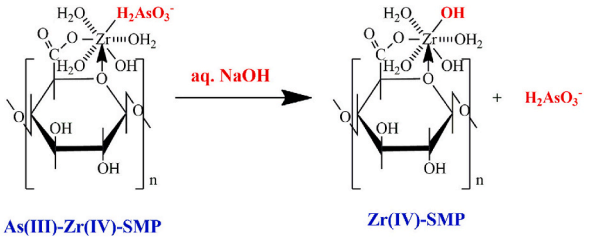

Scheme 3. Mechanism of As(III) desorption using NaOH solution.

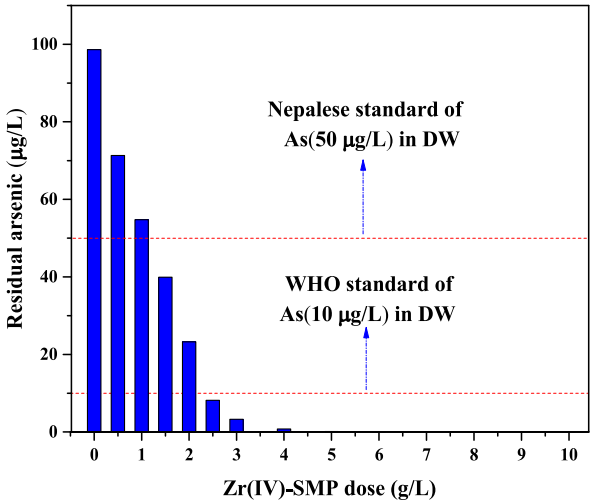

Fig. 9. Application of investigated Zr(IV)-SMP for the removal of arsenic from arsenic-polluted water.

4. Conclusions

The dried powder of RMP was first saponified with $Ca(OH)_2$ and loaded with Zr(IV) to form Zr(IV)-SMP for As(III) scavenging from water. The exchangeable proton in SMP was calculated to be 2.63 mol H+/kg from mass titration. The amounts of various functional

groups such as carboxylic, lactonic, and phenolic were evaluated to be 2.5, 1.85, and 2.80 mol/kg, respectively, using Boehm's titration. The optimum equilibrium pH and contact time for Zr(IV)-SMP were determined to be 10.18 and 6 h, respectively. The experimental data of As(III) scavenging by Zr(IV)-SMP were fitted to the Langmuir isotherm and PSO kinetic models, respectively, which were further confirmed by non-linear fitting. A trace amount of arsenic that existed in contaminated groundwater was successfully lowered down to the WHO drinking water standard by using 2.5 g/L of investigated Zr(IV)-SMP. A comparative study of the maximum As(III) removal capacity of different reported biosorbents with investigated Zr(IV)-SMP shows that Zr(IV)-SMP is a competitive and effective material for As(III) scavenging in aaqueous medium. The interfering effect of commonly co-existing anions (such as sulphate, chloride, and nitrate) during As(III) scavenging shows that sulphate showed a significant reduction in the As(III) scavenging percentage of Zr(IV)-SMP. Effective desorption of As(III) from As(III)–Zr(IV)-SMP could be done using 2M NaOH for its regeneration. Therefore, the Zr(IV)-SMP investigated in this study might be utilized to treat polluted water containing trace amounts of arsenic ions.

Data availability

Data will be made available at a resonable request.

CRediT authorship contribution statement

Deepak Gyawali: Writing – review & editing, Writing – original draft. **Samjhana Poudel:** Writing – original draft, Data curation. **Madan Poudel:** Data curation. **Kedar Nath Ghimire:** Writing – review & editing. **Megh Raj Pokhrel:** Writing – review & editing. **Prabin Basnet:** Writing – review & editing. **Krishna Bahadur BK:** Data curation. **Hari Paudyal:** Conceptualization.

Declaration of competing interest

The authors declare that they have no known competing financial interests or personal relationships that could have appeared to influence the work reported in this paper.

Acknowledgement

The authors of this paper are grateful to Dr. Khag Raj Sharma & Dr. Sabita Shrestha for FTIR measurement and Dr. Bipeen Dahal for recording SEM images, elemental mapping, and EDS spectra of the samples.

Appendix A. Supplementary data

Supplementary data to this article can be found online at https://doi.org/10.1016/j.heliyon.2024.e36496.

References

[1] S.R. Mishra, P. Roy, V. Gadore, M. Ahmaruzzaman, "A combined experimental and modeling approach to elucidate the adsorption mechanism for sustainable water treatment via In2S3-anchored chitosan," Scientific Report, Sci. Rep. 13 (1) (2023) 18051.
[2] M.S. Rahaman, A. Basu, M.R. Islam, The removal of As(III) and As(V) from aqueous solutions by waste materials, Bioresour. Technol. 99 (8) (2008) 2815–2823.
[3] V.K. Sharma, M. Sohn, Aquatic arsenic: toxicity, speciation, transformations, and remediation, Environ. Int. 35 (4) (2009) 743–759.
[4] J.-Y. Chung, S.-D. Yu, Y.-S. Hong, Environmental source of arsenic exposure, Journal of Preventive Medicine and Public Health 47 (5) (2014) 253.
[5] S.R. Mishra, V. Gadore, M. Ahmaruzzaman, Insights into persulfate-activated photodegradation of tinidazole and photoreduction of hexavalent chromium through β-In2S3 anchored on Ag-doped fish scale-derived HAp composite quantum dots, J. Clean. Produc. 427 (2023) 139221.
[6] D. Gyawali, S. Rijal, P. Basnet, K.N. Ghimire, M.R. Pokhrel, H. Paudyal, Effective biosorption of As(V) from polluted water using Fe(III)-modified Pomelo (Citrus maxima) peel: a batch, column, and thermodynamic study, Heliyon 9 (2) (2023) e02023.
[7] M. Shahid, C. Dumat, N. Khan Niazi, S. Khalid, Global scale arsenic pollution: increase the scientific knowledge to reduce human exposure, VertigO-la revue électronique en sciences de l'environnement (Hors-série 31) (2018).
[8] N. Ullah Khan, M. Shahid, S. Khalid, N. Natasha, Z.A. Alothman, A.A. Al-Kahtani, M. Imran, Behzad Murtaza, Arsenic level in groundwater and biological samples in Khanewal, Pakistan, Environ. Geochem. Health 45 (2023) 8943–8952.
[9] W. Ali, A. Rasool, M. Junaid, H. Zhang, A comprehensive review on current status, mechanism, and possible sources of arsenic contamination in groundwater: a global perspective with prominence of Pakistan scenario, Environ. Geochem. Health 41 (2019) 737–760.
[10] S. Lamichhane, A.K. Singh, Analysis of Arsenic Concentration in the Constructed Groundwater of Nepal, 2019.
[11] J.K. Thakur, R.K. Thakur, A. Ramanathan, M. Kumar, S.K. Singh, Arsenic contamination of groundwater in Nepal:- an overview, Water 3 (1) (2010) 1–20.
[12] R. Johnston, H. Heijnen, P. Wurzel, Chapter 6: Safe Water Technology, 2001.
[13] H. Cui, Q. Li, S. Gao, J.K. Shang, Strong adsorption of arsenic species by zirconium oxide nanoparticle, J. Ind. Eng. Chem. 18 (2012) 1418–1427.
[14] A.S. Matharu, J.A. Houghton, C. Lucas-Torres, A. Moreno, Acid-free microwave-assisted hydrothermal extraction of pectin and porous cellulose from mango peel waste – towards a zero waste mango biorefinery, Green Chem. 18 (19) (2016) 5280–5287.
[15] M. Iqbal, A. Saeed, S.I. Zafar, FTIR spectrophotometry, kinetics and adsorption isotherms modelling, ion exchange, and EDX analysis for understanding the mechanism of Cd^{2+} and Pb^{2+} removal by mango peel waste, J. Hazard Mater. 164 (1) (2009) 161–171.
[16] S.L. Goertzen, K.D. Thériault, A.M. Oickle, A.C. Tarasuk, H.A. Andreas, Standardization of the Boehm titration. Part I. CO_2 expulsion and endpoint determination, Carbon 48 (4) (2010) 1252–1261.
[17] D. Mohanta, Md Ahmaruzzaman, Bio-inspired adsorption of arsenite and fluoride from aqueous solutions using activated carbon@SnO_2 nanocomposites: isotherms, kinetics, thermodynamics, cost estimation and regeneration studies, J. Environ. Chem. Eng. 6 (1) (2018) 356–366.

[18] V.J. Vilar, C.M. Botelho, R.A. Boaventura, Copper desorption from Gelidium algal biomass, Water Res. 41 (7) (2007) 1569–1579.
[19] B.R. Poudel, et al., Agro-waste derived biomass impregnated with TiO_2 as a potential adsorbent for removal of As(III) from water, Catalysts 10 (10) (2020) 1125.
[20] R.T. Morrison, Organic Chemistry, Pearson Education India, 1972.
[21] J. García Raurich, A. Vázquez Ricart, M. Pallarès Andreu, P. Monagas Asensio, M.P. Almajano Pablos, Application of citrus bioadsorbents as wine clarifiers, International Journal of Environmental & Agriculture Research (IJOEAR) 5 (3) (2019) 1–11.
[22] A.K. Prajapati, M.K. Mondal, Hazardous As(III) removal using nanoporous activated carbon of waste garlic stem as adsorbent: kinetic and mass transfer mechanisms, Kor. J. Chem. Eng. 36 (11) (2019) 1900–1914.
[23] R.L. Aryal, et al., Effective biosorption of arsenic from water using La(III) loaded carboxyl functionalized watermelon rind, Arab. J. Chem. 15 (3) (2022) 103674.
[24] M. Chiban, M. Zerbet, G. Carja, F. Sinan, Application of low-cost adsorbents for arsenic removal: a review, J. Environ. Chem. Ecotoxicol. 4 (2012) 91–102.
[25] B.K. Biswas, et al., Adsorptive removal of As(V) and As(III) from water by a Zr(IV)-loaded orange waste gel, J. Hazard Mater. 154 (1–3) (2008) 1066–1074.
[26] H. Paudyal, et al., Adsorptive removal of fluoride from aqueous solution using orange waste loaded with multi-valent metal ions, J. Hazard Mater. 192 (2) (2011) 676–682.
[27] S. Zafar, N. Khalid, M. Daud, M.L. Mirza, Kinetic studies of the adsorption of thorium ions onto rice husk from aqueous media: linear and nonlinear approach, Nucleus 52 (1) (2015) 14–19.
[28] P.L. Homagai, K.N. Ghimire, K. Inoue, Preparation and characterization of charred xanthated sugarcane bagasse for the separation of heavy metals from aqueous solutions, Separ. Sci. Technol. 46 (2) (2010) 330–339.
[29] I. Langmuir, The constitution and fundamental properties of solids and liquids, J. Am. Chem. Soc. 38 (1916) 2221–2295, https://doi.org/10.1021/ja02268a002.
[30] H. Freundlich, Uber die adsorption in losungen, J. Phys. Chem. 5 7 (1906) 385–470.
[31] M.B. Shakoor, et al., Exploring the arsenic removal potential of various biosorbents from water, Environ. Int. 123 (2019) 567–579.
[32] P. Bhattarai, K.P. Bohara, M.R. Pokhrel, Adsorptive removal of As(III) from aqueous solution, Journal of Institute of Science and Technology 19 (1) (2014) 150–154.
[33] W.A. Shaikh, et al., Enhanced aqueous phase arsenic removal by a biochar based iron nanocomposite, Environmental Technology & Innovation 19 (2020) 100936.
[34] S. Ali, M. Rizwan, M.B. Shakoor, A. Jilani, R. Anjum, High sorption efficiency for as (III) and As(V) from aqueous solutions using novel almond shell biochar, Chemosphere 243 (2020) 125330.
[35] L. Verma, M.A. Siddique, J. Singh, R.N. Bharagava, As(III) and As(V) removal by using iron impregnated biosorbents derived from waste biomass of Citrus limmeta (peel and pulp) from the aqueous solution and ground water, J. Environ. Manag. 250 (2019) 109452.
[36] W.A.H. Altowayti, H.A. Algaifi, S.A. Bakar, S. Shahir, The adsorptive removal of As(III) using biomass of arsenic resistant Bacillus thuringiensis strain WS3: characteristics and modelling studies, Ecotoxicol. Environ. Saf. 172 (2019) 176–185.
[37] S. Mandal, M.K. Sahu, R.K. Patel, Adsorption studies of arsenic(III) removal from water by zirconium polyacrylamide hybrid material (ZrPACM-43), Water Resour. Ind. 4 (2013) 51–67.
[38] A.S. Gugushe, A. Nqombolo, P.N. Nomngongo, Application of response surface methodology and desirability function in the optimization of adsorptive remediation of arsenic from acid mine drainage using magnetic nanocomposite: equilibrium studies and application to real samples, Molecules 24 (9) (2019) 1792.
[39] I.L. Ouma, E.B. Naidoo, A.E. Ofomaja, Thermodynamic, kinetic and spectroscopic investigation of arsenite adsorption mechanism on pine cone-magnetite composite, J. Environ. Chem. Eng. 6 (4) (2018) 5409–5419.
[40] S. Sert, A. Celik, V.N. Tirtom, Removal of arsenic(III) ions from aqueous solutions by modified hazelnut shell, Desalination Water Treat. 75 (2017) 115–123.
[41] B.R. Vieira, A.M. Pintor, R.A. Boaventura, C.M. Botelho, S.C. Santos, Arsenic removal from water using iron-coated seaweeds, J. Environ. Manag. 192 (2017) 224–233.
[42] L. Hao, T. Zheng, J. Jiang, G. Zhang, P. Wang, Removal of As(III) and As(V) from water using iron doped amino functionalized sawdust: characterization, adsorptive performance and UF membrane separation, Chem. Eng. J. 292 (2016) 163–173.
[43] D. Setyono, S. Valiyaveettil, Chemically modified sawdust as renewable adsorbent for arsenic removal from water, ACS Sustain. Chem. Eng. 2 (12) (2014) 2722–2729.
[44] P.K. Pandey, S. Choubey, Y. Verma, M. Pandey, K. Chandrashekhar, Biosorptive removal of arsenic from drinking water, Bioresour. Technol. 100 (2) (2009) 634–637.
[45] S. Luther, N. Borgfeld, J. Kim, J.G. Parsons, Removal of arsenic from aqueous solution: a study of the effects of pH and interfering ions using iron oxide nanomaterials, Microchem. J. 101 (2012) 30–36.
[46] Y. John, V.E. David, D. Mmereki, A comparative study on removal of hazardous anions from water by adsorption: a review, Int. J. Chem. Eng. 2018 (2018) 1–21.
[47] S. Mandal, M.K. Sahu, R.K. Patel, Adsorption studies of arsenic(III) removal from water by zirconium polyacrylamide hybrid material (ZrPACM-43), Water Resour. Ind. 4 (2013) 51–67.